THE STELLAR MASS COMPONENTS OF GALAXIES:
COMPARING SEMI-ANALYTICAL MODELS WITH OBSERVATION

Lei Liu[1,5], Xiaohu Yang[1], H.J. Mo [2], Frank C. van den Bosch[3], Volker Springel[4]
Draft version February 8, 2010

ABSTRACT

We compare the stellar masses of central and satellite galaxies predicted by three independent semi-analytical models with observational results obtained from a large galaxy group catalogue constructed from the Sloan Digital Sky Survey. In particular, we compare the stellar mass functions of centrals and satellites, the relation between total stellar mass and halo mass, and the conditional stellar mass functions, $\Phi(M_*|M_h)$, which specify the average number of galaxies of stellar mass M_* that reside in a halo of mass M_h. The semi-analytical models only predict the correct stellar masses of central galaxies within a limited mass range and all models fail to reproduce the sharp decline of stellar mass with decreasing halo mass observed at the low mass end. In addition, all models over-predict the number of satellite galaxies by roughly a factor of two. The predicted stellar mass in satellite galaxies can be made to match the data by assuming that a significant fraction of satellite galaxies are tidally stripped and disrupted, giving rise to a population of intra-cluster stars in their host halos. However, the amount of intra-cluster stars thus predicted is too large compared to observation. This suggests that current galaxy formation models still have serious problems in modeling star formation in low-mass halos.

Subject headings: dark matter - large-scale structure of universe - galaxies: halos

1. INTRODUCTION

Semi-analytical models (hereafter SAMs) are a powerful method to study the formation and evolution of galaxies in a CDM cosmogony (e.g., White & Frenk 1991; Lacey et al. 1991; Kauffmann et al. 1993; Cole et al. 1994, 2000; Somerville et al. 1999; Benson et al. 2000). Since dark matter couples to baryons only through gravity, the galaxy formation process is expected to only have a small effect on the dark matter distribution. Tests using N-body and hydrodynamical simulations (with and without star formation) have shown that the general properties of the large scale structure, such as the overall structure and distribution of dark matter halos, are not significantly affected by gas physics (e.g. Lin et al. 2006). It is therefore possible to separate the modeling of galaxy formation and evolution into two steps: (i) modeling the formation and evolution of the halo population using either N-body simulations or (semi)-analytical methods (i.e., extended Press-Schechter theory), and (ii) modeling how galaxies form and evolve within individual dark matter halos using a semi-analytical approach. In the second step, one incorporates various physical processes, such as gas cooling, star formation and feedback, to predict the properties of the galaxy population.

The advantage of this semi-analytical approach compared to, for example, full hydrodynamical simulations is

that it allows a relatively fast and flexible exploration of a large parameter space. Typically, the free parameters that describe the efficiencies of cooling, star formation and feedback are tuned to reproduce certain (global) observational constraints, such as the luminosity function, the Tully-Fisher relation and the color-magnitude relation, among others. In the past decade this technique has been used extensively to constrain the various physical processes that play a role in the formation and evolution of galaxies, and to make predictions for future observations (e.g., Kauffmann et al. 1999; Helly et al. 2003; Kang et al. 2005; Bower et al. 2006; Croton et al. 2006; Cattaneo et al. 2006; De Lucia & Blaizot 2007; Monaco, Fontanot & Taffoni 2007; Henriques, Bertone & Thomas 2008; Somerville et al. 2008; Neistein & Weinmann 2009).

So far, however, in most of the SAMs, only global properties of the galaxy population have been used extensively and consistently as constraints on their free parameters. Although reproducing these global properties is clearly an important first step, it lacks the power to constrain model assumptions in detail. For example, a model may overestimate the galaxy population in some (e.g. massive) halos while underestimating that in other halos, or overestimate the stellar mass in central galaxies while underestimating that in satellites, and yet match the total stellar mass function.

In recent years, much progress has been made in constraining the properties of galaxies as function of halo mass. For example, numerous authors have used the clustering properties of galaxies in order to constrain the halo occupation distribution (HOD), $P(N|M_h)$, which specifies the probability that a halo of mass M_h contains N galaxies (e.g., Jing, Mo & Börner 1998; Scranton 2003; Zehavi et al. 2004, 2005; Tinker et al. 2005; Collister & Lahav 2005; Zheng et al. 2005; 2007; Tinker & Wetzel 2009) or the conditional luminosity function (CLF), $\Phi(L|M_h)dL$, which specifies the average number of galax-

[1] Key Laboratory for Research in Galaxies and Cosmology, Shanghai Astronomical Observatory; the Partner Group of MPA; Nandan Road 80, Shanghai 200030, China; E-mail: liulei@shao.ac.cn
[2] Department of Astronomy, University of Massachusetts, Amherst MA 01003-9305
[3] Department of Physics and Astronomy, University of Utah, 115 South 1400 East, Salt Lake City, UT 84112-0830
[4] Max-Planck-Institut für Astrophysik, Karl-Schwarzschild-Strasse 1, 85748 Garching, Germany
[5] Graduate School of the Chinese Academy of Sciences, 19A, Yuquan Road, Beijing, China

ies of luminosity $L \pm dL/2$ that reside in a halo of mass $M_{\rm h}$ (e.g., Yang, Mo & van den Bosch 2003; van den Bosch, Yang & Mo 2003; Cooray 2006; van den Bosch et al. 2007; Cacciato et al. 2009). These statistics provide detailed information about how galaxies of different luminosities (or stellar masses) are connected to dark matter halos of different masses, and can therefore put more stringent constraints on models of galaxy formation and evolution.

However, as pointed out by Yang et al. (2005b), one disadvantage of these HOD/CLF models is that the results are not completely model independent, i.e. one typically has to postulate a functional form for either $P(N|M_{\rm h})$ or $\Phi(L|M_{\rm h})$. This problem can be circumvented by using galaxy group catalogues. If galaxy groups are defined as the ensembles of galaxies that reside in the same dark matter host halo, these group catalogues yield a much more direct probe of the galaxy-dark halo connection. With this in mind, Yang et al. (2005a) developed an adaptive halo-based group finder that can properly link galaxies according to their common dark matter halos. Yang et al. (2007) applied this halo-based group finder to the Sloan Digital Sky Survey (SDSS) Data Release 4 (Adelman-McCarthy et al. 2006), and used the resulting group catalogues to infer the conditional luminosity functions (CLF) and the conditional stellar mass functions (CSMF) directly from the data, separately for central and satellite galaxies (Yang et al. 2008, 2009b; hereafter Y09b). Especially the ability to split the galaxy population in centrals and satellites is an important advantage of using group catalogues. After all, from the point of view of galaxy formation, central and satellite galaxies are subjected to very different processes: whereas central galaxies are believed to reside at the centers of their dark matter halos, where they cannibalize satellite galaxies that have lost their momentum due to dynamical friction, and act as the recipients of new gas via cooling flows, satellite galaxies orbit around central galaxies and are subjected to a number of satellite-specific processes, such as tidal stripping and heating, ram-pressure stripping, galaxy harassment, and strangulation. Consequently, central and satellite galaxies of a given stellar mass are expected to have different properties, something that has recently been confirmed observationally using the SDSS group catalogues of Y07 (e.g., van den Bosch et al. 2008; Pasquali et al. 2009a,b; Weinmann et al. 2006a, 2009; Skibba 2009).

A comparison of the halo occupation statistics obtained from these galaxy group catalogues with predictions from semi-analytical models has already provided important new insights into galaxy formation and evolution. Weinmann et al. (2006b) and Kimm et al. (2009) compared the color distributions of central and satellite galaxies in halos of different masses to predictions from various semi-analytical models, and showed that the latter dramatically over-predict the red fraction of satellite galaxies. This problem has become known as the over-quenching problem, and has triggered a number of studies into the mechanisms that may cause quenching of star formation in satellite galaxies (e.g., Baldry et al. 2006; Kang & van den Bosch 2008; Font et al. 2008; Mc-Carthy et al. 2008; van den Bosch et al. 2008; Fontanot et al. 2009; Weinmann et al. 2009). Yang et al. (2009a; hereafter Y09a) used the CSMF obtained from the group catalogues to discuss the fate of satellite galaxies, and

suggested that a significant fraction is likely to be tidally disrupted after being accreted into their host halos, producing a population of intra-cluster stars. Pasquali et al. (2009b) studied the ages and metallicities of central and satellite galaxies as functions of both stellar mass and halo mass, and showed that the SAM of Wang et al. (2008), which predicts stellar mass functions and two-point correlation functions in good overall agreement with observations, fails to reproduce the halo mass dependence of the metallicities of low mass satellites, and predicts that satellite galaxies have the same metallicities as centrals of the same stellar mass, in disagreement with the data. In agreement with Y09a, they argue that this is likely to reflect the impact of satellite disruption, a process that has almost never been included in semi-analytical models thus far (but see Benson et al. 2002).

In this paper we make use of the various stellar mass functions of central and satellite galaxies in halos of different masses obtained by Y09b to evaluate three recent SAMs carried out by Kang et al. (2005), Bower et al. (2006) and De Lucia & Blaizot (2007). This paper is organized as follows. In §2 we outline the main properties of the SDSS DR4 galaxy group catalogues. §3 gives a brief description of the semi-analytical models used in this paper, highlighting their similarities as well as their differences. In §4, we describe the construction of mock galaxy redshift surveys and the corresponding mock group catalogues. In §5 we compare the galaxy stellar mass functions, the relation between total stellar mass and halo mass, and the conditional stellar mass functions predicted by the semi-analytical models with the results from the Y07 group catalogue. We discuss the implications of this comparison in §6, and summarize our results in §7.

Throughout this paper we adopt a ΛCDM cosmology with parameters that are consistent with the three-year data release of the WMAP mission (hereafter WMAP3 cosmology): $\Omega_{\rm m} = 0.238$, $\Omega_{\Lambda} = 0.762$, $\Omega_{\rm b} = 0.042$, $n = 0.951$, $h = H_0/(100\,{\rm km\,s^{-1}\,Mpc^{-1}}) = 0.73$ and $\sigma_8 = 0.75$ (Spergel et al. 2007). Wherever necessary, we have converted the halo masses to this particular cosmology using abundance matching based on the halo mass functions. Note however, we did not adjust any galaxy properties accroding to the updated halo masses, i.e., re-run the SAMs. Since SAMs are constrained using the global properties of galaxies, we expect that the change will be small and not impact any of our results significantly.

2. GALAXY GROUPS IN SDSS DR4

The observational data used here are galaxy group catalogues constructed from the New York University Value-Added Galaxy Catalogue (NYU-VAGC; Blanton et al. 2005), which is based on the SDSS Data Release 4 (Adelman-McCarthy et al. 2006). From this NYU-VAGC Y07 selected all galaxies in the Main Galaxy Sample with an extinction corrected apparent magnitude brighter than $r = 18$, with redshifts in the range $0.01 \leq z \leq 0.20$ and with a redshift completeness $\mathcal{C}_z > 0.7$. This sample of galaxies is used to construct three group samples: sample I, which only uses the 362,356 galaxies with measured redshifts from the SDSS, sample II which also includes 7,091 galaxies with SDSS photometry but with

redshifts taken from alternative surveys, and sample III which includes an additional 38,672 galaxies that lack a redshift due to fiber-collisions, but which we assign the redshift of its nearest neighbor (cf. Zehavi et al. 2002). The analysis presented in this paper is mainly based on sample II. Survey edge effects have been taken into account by removing those groups (about 1.6% of the total) that are too close to one of the edges of the survey. The stellar mass, M_*, of each galaxy is computed using the relations between stellar mass-to-light ratio and $^{0.0}(g-r)$ color from Bell et al. (2003),

$$\log \left[\frac{M_*}{h^{-2}\,\mathrm{M}_\odot} \right] = -0.306 + 1.097 \left[^{0.0}(g-r) \right] - 0.10$$
$$-0.4 (^{0.0}M_r - 5\log h - 4.64). \qquad (1)$$

Here $^{0.0}(g-r)$ and $^{0.0}M_r - 5\log h$ are the $g-r$ color and r-band magnitude $K+E$-corrected to $z=0$, respectively, the number 4.64 is the r-band magnitude of the Sun in the AB system (Blanton & Roweis 2007), and the -0.10 term reflects the assumption of a Kroupa (2001) IMF.

Galaxies are split into "centrals", which are defined as the most massive group members in terms of their stellar mass, and "satellites", which are those group members that are not centrals. For each group in the Y07 catalogue two estimates of its dark matter halo mass, M_h, are available: one based on the ranking of its total characteristic luminosity, and the other based on the ranking of its total characteristic stellar mass. Both halo masses agree very well with each other, with an average scatter that decreases from ~ 0.1 dex at the low mass end to ~ 0.05 dex at the massive end. With the method of Y07, halo masses can only be assigned to groups more massive than $\sim 10^{12}h^{-1}\mathrm{M}_\odot$ which have at least one member with $^{0.1}M_r - 5\log h \leq$ -19.5 mag. For smaller mass halos, Yang et al. (2008) have used the relations between the luminosity (stellar mass) of central galaxies and the halo mass of their groups to extrapolate the halo mass of single central galaxies down to $M_\mathrm{h} \simeq 10^{11}h^{-1}\,\mathrm{M}_\odot$. This extends the number of galaxies with an assigned halo mass from 295,861 in the original Y07 paper to all 369,447 galaxies in sample II.

Due to the flux limit of the survey, only galaxies brighter than a certain magnitude can be observed. This induces incompleteness in the stellar masses of galaxies and the halo masses of groups. As shown in the Appendix of van den Bosch et al. (2008), for the stellar masses of galaxies, the apparent magnitude limit of the galaxy sample, $m_r = 17.77$, can be translated to a stellar mass limit as function of redshift z:

$$\log[M_{*,\mathrm{lim}}/(h^{-2}\,\mathrm{M}_\odot)] = \qquad (2)$$
$$\frac{4.852 + 2.246\log D_L(z) + 1.123\log(1+z) - 1.186z}{1 - 0.067z}.$$

The galaxy sample is complete for galaxies with $M_* \geq M_{*,\mathrm{lim}}$. As shown in Y09b, the corresponding halo mass limit at z, $\log M_{\mathrm{h,lim}}$, is given by

$$\log M_{\mathrm{h,lim}} = (z - 0.085)/0.069 + 12. \qquad (3)$$

The group catalogue is complete for groups with $M_\mathrm{h} \geq M_{\mathrm{h,lim}}$. Taking these two mass limits into account, Y09b measured various stellar mass functions for galaxies and groups, including the conditional stellar mass functions $\Phi(M_*|M_\mathrm{h})$. In this paper we use these statistics to evaluate the three independent semi-analytical models described below.

3. SEMI-ANALYTICAL MODELS

The first semi-analytical model to be considered is the one presented in De Lucia & Blaizot (2007; hereafter D07), which uses the methods developed by Kauffmann & Haehnelt (2000), Springel et al. (2001) and De Lucia et al. (2006). This model is a modified version of that presented in Croton et al. (2006), and includes a prescription for the growth and activity of central black holes and their effect on suppressing the cooling and star formation in massive halos. D07 use the initial mass function (IMF) of Chabrier (2003), in contrast to Croton et al. (2006), who adopted a Salpeter IMF. The total number of galaxies (centrals plus satellites) in this catalogue is 25,801,944, distributed within a total of 14,752,323 dark matter halos.

The second semi-analytical model used in this paper is taken from Bower et al. (2006; hereafter B06). This model uses the Durham semi-analytical model GAL-FORM, which is described in detail in Cole et al. (2000) and Benson et al. (2003), but has several additional features, including the formation and growth of black holes, AGN feedback, and disk instability (see B06 for details). This model adopts a Kennicutt (1983) IMF with no correction for brown dwarf stars. The catalogue of model galaxies consists of 24,569,785 galaxies distributed over 10,957,827 dark matter halos.

The third and final semi-analytical to be considered in this paper is that of Kang et al. (2005; hereafter K05). Unlike the previous two models it does not include AGN feedback. K05 adopted both a Salpeter IMF and a Scalo IMF, and found that by adjusting model parameters, the results for the two IMFs are very similar. The K05 catalogue of model galaxies has 752,241 entries distributed over 399,983 halos.

All three SAMs share many basic properties. They are all based on dark matter halo merging trees obtained directly from N-body simulations, Models D07 and B06 are based on the Millennium Run N-body simulation (Springel et al. 2005b), a large dark-matter-only simulation of the ΛCDM cosmology with $2160^3 \simeq 1.0078 \times 10^{10}$ particles in a periodic box of $500h^{-1}$Mpc on a side. The mass of each particle is $8.6 \times 10^8\,h^{-1}\mathrm{M}_\odot$, and the smallest halos identified consist of about 20 particles. The simulation was carried out using a special version of the GADGET-2 code (Springel et al. 2005a). The simulation used in K05 was carried out using the vectorized parallel P^3M code of Jing & Suto (2002) with 512^3 particles distributed over a box $100h^{-1}$Mpc on a side. The particle mass is $6.2 \times 10^8h^{-1}\,\mathrm{M}_\odot$. To identify substructures in the halos, all three SAMs used the routine SUBFIND developed by Springel et al. (2001). Note that each model used a slightly different approach to construct their halo merger trees, which may affect the properties of the resulting galaxies. Details can be found in the papers presenting each individual model. As is standard in semi-analytical models, all three models considered here take into account basic physical processes, such as gas cooling, star formation, supernova feedback, galaxy mergers, and chemical enrichment. Following White & Frenk (1991),

they all define a cooling radius and compare it with another critical radius to separate the static hot halo regime from the rapid cooling regime: in D07 and K05 this is the virial radius $r_{\rm vir}$, while B06 use the free-fall radius $r_{\rm ff}$ instead. As mentioned above, both D07 and B06 include AGN feedback to suppress cooling flows in massive halos, and both are based on the AGN model of Kauffmann & Haehnelt (2000), though the detailed implementations are different (see below). Finally, both D07 and B06 took into account the effects of re-ionization of the universe. In B06, gas cooling is assumed to be completely suppressed in dark matter halos with virial velocities below $50\,{\rm km\,s^{-1}}$ at redshifts below $z = 6$, while in D07, the effect of photoionization heating is assumed to reduce the gas fraction from the universal value $f_{\rm b}^{\rm cosmic}$ to

$$f_{\rm b}^{\rm halo}(z, M_{\rm vir}) = \frac{f_{\rm b}^{\rm cosmic}}{[1 + 0.26 M_{\rm F}(z)/M_{\rm vir}]^3}\,, \qquad (4)$$

where $M_{\rm vir}$ is the virial mass of the halo in question, and $M_{\rm F}$ is a filtering mass (e.g., Gnedin 2000).

Note that the K05 model does not include AGN feedback nor reionization. Nevertheless, as we show in section 5 below, in terms of the stellar mass distributions, the K05 yields results that are very comparable to those of D07 and B06. In the following two subsections we highlight a few of the differences between the three SAMs considered here that may have a significant impact on the outcome of the stellar masses of the model galaxies.

3.1. Black hole growth and AGN feedback

D07 follow the treatment of AGN activity described in Croton et al. (2006). Central massive black holes grow through two modes: the *quasar mode* and the *radio mode*. In the quasar mode, black holes grow during galaxy mergers. The gas mass accreted during the merger is assumed to be proportional to the total cold gas mass, but with a lower efficiency for smaller mass systems:

$$\Delta m_{\rm BH,Q} = \frac{f'_{\rm BH} m_{\rm cold}}{1 + (280{\rm km\,s^{-1}}/V_{\rm vir})^2} \qquad (5)$$

where $f'_{BH} = f_{BH} \times (m_{\rm sat}/m_{\rm cen})$ and $f_{\rm BH} \approx 0.03$ is a constant. Black hole accretion is allowed both in major and minor mergers, and the efficiency is assumed to be proportional to the mass ratio of the merging galaxies, $m_{\rm sat}/m_{\rm cen}$. In the radio mode, the AGN activity is assumed to be powered by accretion of hot gas onto the central black hole, and the accretion rate is assumed to be

$$\dot{m}_{\rm BH,R} = \kappa_{\rm AGN} \left(\frac{m_{\rm BH}}{10^8\,{\rm M_\odot}}\right) \left(\frac{f_{\rm hot}}{0.1}\right) \left(\frac{V_{\rm vir}}{200{\rm km\,s^{-1}}}\right)^3 \qquad (6)$$

where $m_{\rm BH}$ is the black hole mass, $f_{\rm hot}$ is the fraction of the total halo mass in the form of hot gas and the free parameter $\kappa_{\rm AGN}$ is set to be $6 \times 10^{-6}\,{\rm M_\odot yr^{-1}}$. It is assumed that the black hole growth during the radio-mode results in AGN feedback which strongly suppresses the cooling of hot gas in massive halos[6]. As shown in Croton et al. (2006), this radio-mode AGN feedback has

---

[6] Note that the model does *not* incorporate any direct feedback, be it hydrodynamical or radiative, from the quasar-mode accretion.

the effect that it completely stops cooling in halos with $V_{\rm vir} \gtrsim 300{\rm km\,s^{-1}}$ between $z = 1$ and the present. In fact, AGN feedback is considered to provide a physical 'explanation' for the treatment of gas cooling in early semi-analytical models. For instance, Kauffmann et al. (1999) assume that gas cooling is absent in halos with $V_{\rm vir} > 350{\rm km\,s^{-1}}$. K05 also follow this approach, adopting a slightly higher critical virial velocity of $390{\rm km\,s^{-1}}$. So although they do not incorporate AGN feedback as such, they modify the cooling prescription so that it effectively has a very similar impact.

The treatment of black hole growth in B06 is based on Kauffmann & Haehnelt (2000), and the details can be found in Malbon et al. (2007). Central black holes are assumed to grow through gas accretion triggered by both galaxy mergers and disk instability, and the growth is controlled by an efficiency parameter $F_{\rm BH}$, which is the ratio between the gas mass accreted onto the black hole and that turned into stars during a starburst. Note that in B06, AGN feedback is effective only in halos where a static hot atmosphere has formed. This is defined to be the case when the cooling time is longer than the free-fall time. They assume that only in this case the energy from the central black hole can suppress the cooling flows and thus regulate the cooling rate. Feedback in this scheme is similar to the radio mode considered in Croton et al. (2006), but the details are quite different. B06 simply assume that the AGN power prevents gas from cooling if

$$L_{\rm cool} < \epsilon_{\rm SMBH} L_{\rm Edd}\,, \qquad (7)$$

independent of the gas temperature. In the above expression, $L_{\rm cool}$ is the cooling luminosity, and the available AGN power is parameterized as a fraction $\epsilon_{\rm SMBH}$ of the Eddington luminosity of the central black hole.

3.2. Starburst model

All three models considered here include a prescription for starbursts triggered by major mergers, defined as the merger between the stellar bodies of two galaxies with a mass ratio larger than 0.3. During a major merger, all the stellar mass in the two progenitors is transformed into a spheroidal 'bulge' component, while some or all of the cold gas is assumed to undergo a starburst. In K05 and B06, all the cold gas is assumed to turn into bulge stars, while in D07 they adopt the implementation of Somerville et al. (2001), only a fraction

$$e_{\rm burst} = \beta_{\rm burst}(m_{\rm sat}/m_{\rm cen})^{\alpha_{\rm burst}}\,, \qquad (8)$$

of the cold gas is converted into bulge-stars. Motivated by the numerical simulation results of Cox et al. (2004), D07 chose $\alpha_{\rm burst} = 0.7$ and $\beta_{\rm burst} = 0.56$.

Besides these major-merger induced starbursts, D07 and B06 also include a prescription for starbursts triggered by disk instability. When a galaxy disk is sufficiently massive that its self-gravity is dominant, it is assumed to be unstable to small perturbations. The instability criterion is based on the quantity

$$\epsilon = \frac{V_{\rm max}}{(GM_{\rm disk}/r_{\rm disk})^{1/2}}\,, \qquad (9)$$

where $V_{\rm max}$ is the maximum value of the rotation curve, and $M_{\rm disk}$ and $r_{\rm disk}$ are the mass and scale length of the

disk, respectively. If, at any step, $\epsilon < \epsilon_{\rm disc}$, the disk is assumed to be unstable. In D07, enough stellar mass is transferred to the bulge such that the disk will restore stability. While in B06, the entire mass in the disk will be transferred to the bulge, with any gas present assumed to undergo a starburst (van den Bosch 1998; Mo et al. 1998; Cole et al. 2000; Croton et al. 2006; Bower et al. 2006).

4. MOCK GALAXY REDSHIFT SURVEYS AND GROUPS

The end product of each SAM considered here is a large sample of galaxies distributed over the dark matter halos in a large cubic simulation box. One approach would be to compare these galaxy samples *directly* with the SDSS data. However, this ignores the fact that the latter is affected by observational selection effects, and by inaccuracies related to our halo-based group finder. In particular, the group finder used to identify galaxy groups from the SDSS suffers from incompleteness and from contamination by interlopers (see Yang et al. 2005a, 2007). Furthermore, the halo masses for the SDSS groups are estimated from the ranking of the characteristic luminosities and stellar masses of the groups, which effectively assumes a deterministic (i.e. zero scatter) relation between these quantities and halo mass. In reality there will be non-zero scatter, which results in errors in the inferred halo mass, which are expected to be larger for less massive halos (see Y09b). To test the severity of such effects, we construct mock galaxy redshift surveys (MGRSs) from the D07 and B06 SAM simulation boxes to which we apply our halo-based group finder. Since the box size of the K05 SAM is small ($100\ h^{-1}{\rm Mpc}$), we do not construct a MGRS for this model.

Our construction of the MGRS here is similar to that described in Li et al. (2007a; see also Yang et al. 2004). First, we stack $3 \times 3 \times 3$ replicates of the simulation box and place a virtual observer at the center of the stacked boxes. Next, we assign each galaxy $(\alpha,\ \delta)$-coordinates and remove the ones that are outside the mocked SDSS survey region. For each model galaxy in the survey region, we compute its redshift (which includes the cosmological redshift due to the universal expansion, the peculiar velocity, and a $35\ {\rm km\,s^{-1}}$ Gaussian line-of-sight velocity dispersion to mimic the redshift errors in the data), its r-band apparent magnitude (based on the r-band luminosity of the galaxy), and its absolute magnitude $^{0.1}{\rm M}_r - 5\log h$ which is $K + E$ corrected to $z = 0.1$. For D07, where only absolute magnitudes in vega $UBVRI$ bands are available, we convert them into SDSS g- and r-bands using the relations provided in Fukugita et al. (1996). We eliminate galaxies that are fainter than the SDSS apparent-magnitude limit, and incorporate the position-dependent incompleteness by randomly eliminating galaxies according to the completeness factors obtained from the survey masks provided by the NYU-VAGC (Blanton et al. 2005). Finally we construct group catalogues from the MGRSs for both D07 and B06, using the same halo-based group finder as used for the real SDSS DR4.

Note that in the MGRSs, stellar masses are obtained directly from the SAMs, i.e., they are not obtained from their g- and r-band magnitudes using Eq. 1, as for the SDSS galaxies. The reason is that in SAMs, photometric properties of galaxies are calculated using stellar population synthesis models, using stellar masses taken from these derived magnitudes will introduce addtional uncertainties. For the halo masses, however, we do not use the actual masses of the halos in the SAMs. Rather, we assign each mock group a halo mass based on the ranking of its characteristic stellar masses, in the same way as we assigned halo masses to the SDSS groups.

5. THE STELLAR MASS COMPONENTS OF GALAXY GROUPS

In what follows we compare the predictions of the SAMs described above with the observational results. The quantities to be compared include the global stellar mass functions, the total stellar mass in halos of different masses, and the conditional stellar mass functions.

5.1. *The galaxy stellar mass functions: central versus satellite galaxies*

We start by comparing the stellar mass functions for all, central and satellite galaxies. The results are shown in Fig. 1, where the symbols with errorbars indicate the SDSS data, and the histograms correspond to the different SAMs, as indicated in the upper right-hand panel. The left-hand panels show the model results obtained directly from the cubic SAM simulation boxes, while the right-hand panels show the results obtained from groups selected from the MGRSs (only for D07 and B06).

Comparing the results obtained directly from the cubic boxes (left-hand panels) with those from the MGRSs (right-hand panels), it is evident that the survey selection effects and the contamination due to the group finder do not change any of the results qualitatively. Some small differences are apparent at the low mass end, which partially reflects the fact that the effective survey volume is small and cosmic variance is large.

From the upper left-hand panel of Fig.1 it is clear that the stellar mass functions of galaxies predicted by the three SAMs are roughly consistent with the data in the intermediate stellar mass range ($\log M_* \sim 10.2 - 11.0$). However, all three models significantly over-predict the stellar mass function at the low-mass end. At the high-mass end ($\log M_* \gtrsim 11.0$), D07 slightly over-predicts, B06 slightly under-predicts, and K05 significantly over-predicts the stellar mass function.

In order to examine the discrepancies between model predictions and data in more detail, we next consider the stellar mass functions separately for central and satellite galaxies. As shown in the panels in the second row of Fig. 1, the B06 model is in good agreement with the observed stellar mass function of centrals at the low-mass end, but significantly under-estimates the number density of massive centrals (those with $\log M_* \gtrsim 10.0$). D07 slightly over-predicts the number of central galaxies at the low-mass end, but fairs well at the high-mass end. K05, finally, only reproduces the data in the intermediate mass range. For satellite galaxies (shown in the panels in the third row of Fig. 1), all three SAMs over-predict the number density of satellite galaxies, especially at the low-mass end. The B06 model fairs best, and actually reproduces the number densities of massive satellites, but overall it is clear that the SAMs predict too many satellite galaxies. This is illustrated even more clearly in the lower row of panels of Fig. 1, which show the ratio $\Phi_{\rm s}/\Phi_{\rm c}$
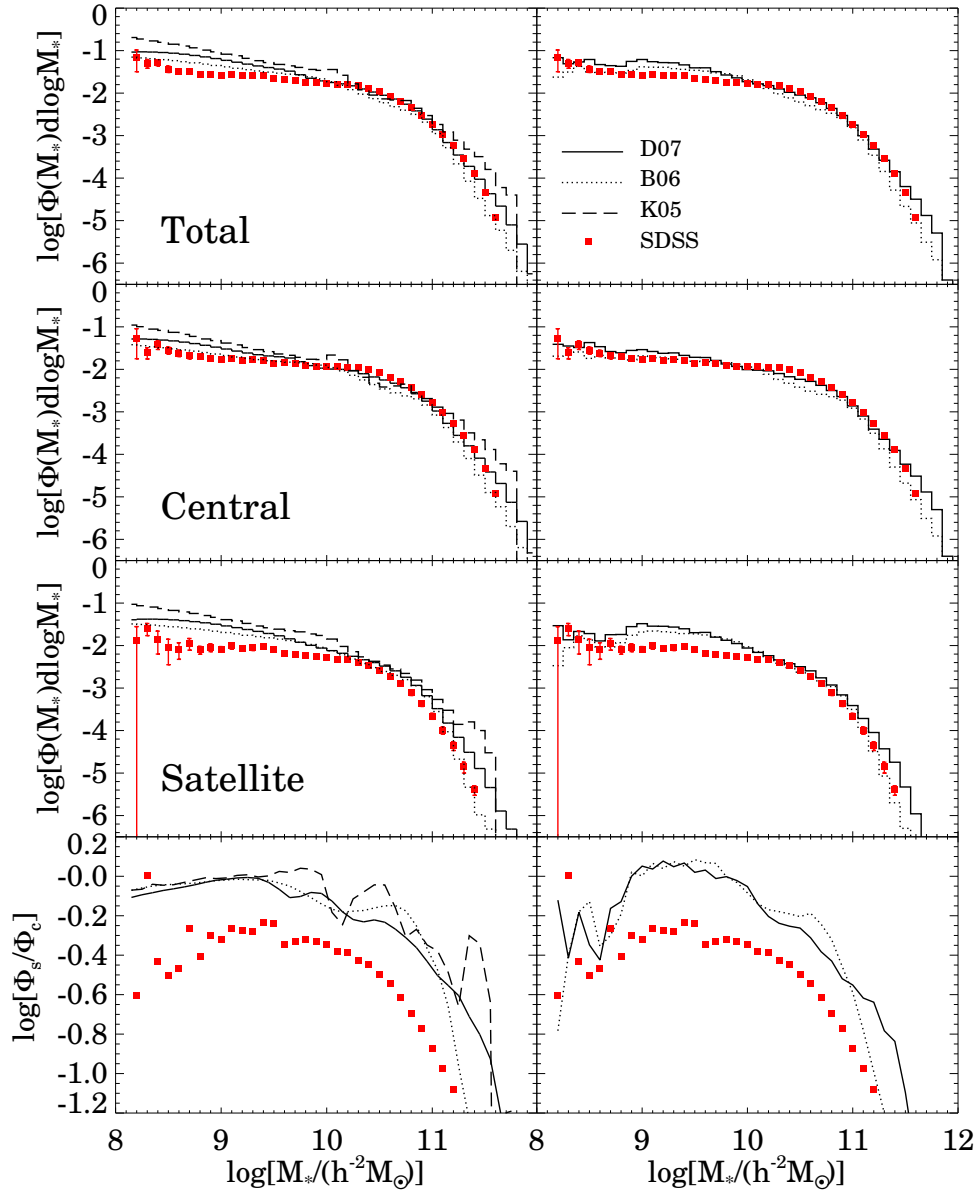
FIG. 1.— Galaxy stellar mass functions. Results shown in the left panels are obtained directly from the SAMs in the cubic boxes, while the right panels are obtained from the galaxy groups extracted from the MGRSs. The first three rows on top show stellar mass functions for all, central and satellite galaxies, respectively. The solid, dotted and dashed histograms are results obtained from the semi-analytical models of D07, B06 and K05, respectively. Since the statistical errors for SAMs are negligible, we do not plot them in the figure. For comparison, symbols with error bars are the SDSS observational data obtained by Y09b. In the bottom row of panels, we show the ratio of Φ_s/Φ_c (third v.s. second panel) for the corresponding SAMs (lines) and SDSS observation (dots), respectively.

of the stellar mass functions of satellite and central galaxies. All three SAMs over-predict this ratio by about a factor of two. The implications of these results are discussed in Section 6.

5.2. The stellar masses of central and satellite galaxies in halos of different masses

In order to look into the origin of the discrepancy between model prediction and observation, Fig.2 shows the total stellar masses of central galaxies (left panel), satellite galaxies (middle panels), and all galaxies (right panels), as functions of the host halo mass. The results obtained directly from the SAM simulation boxes (BOX)

TABLE 1
THE BEST FIT PARAMETERS FOR THE STELLAR MASS FUNCTION OF
CENTRAL GROUP GALAXIES

Source	$\log M_0$	$\log M_1$	α	β
Y09b	10.306	11.040	0.315	4.543
De Lucia & Blaizot (2007; D07)	10.128	11.300	0.451	2.164
Bower et al. (2006; B06)	9.967	11.493	0.466	1.844
Kang et al. (2005; K05)	10.494	11.719	0.401	1.392

NOTE. — M_0 is in units of h^{-2} M$_\odot$ and M_1 in h^{-1} M$_\odot$
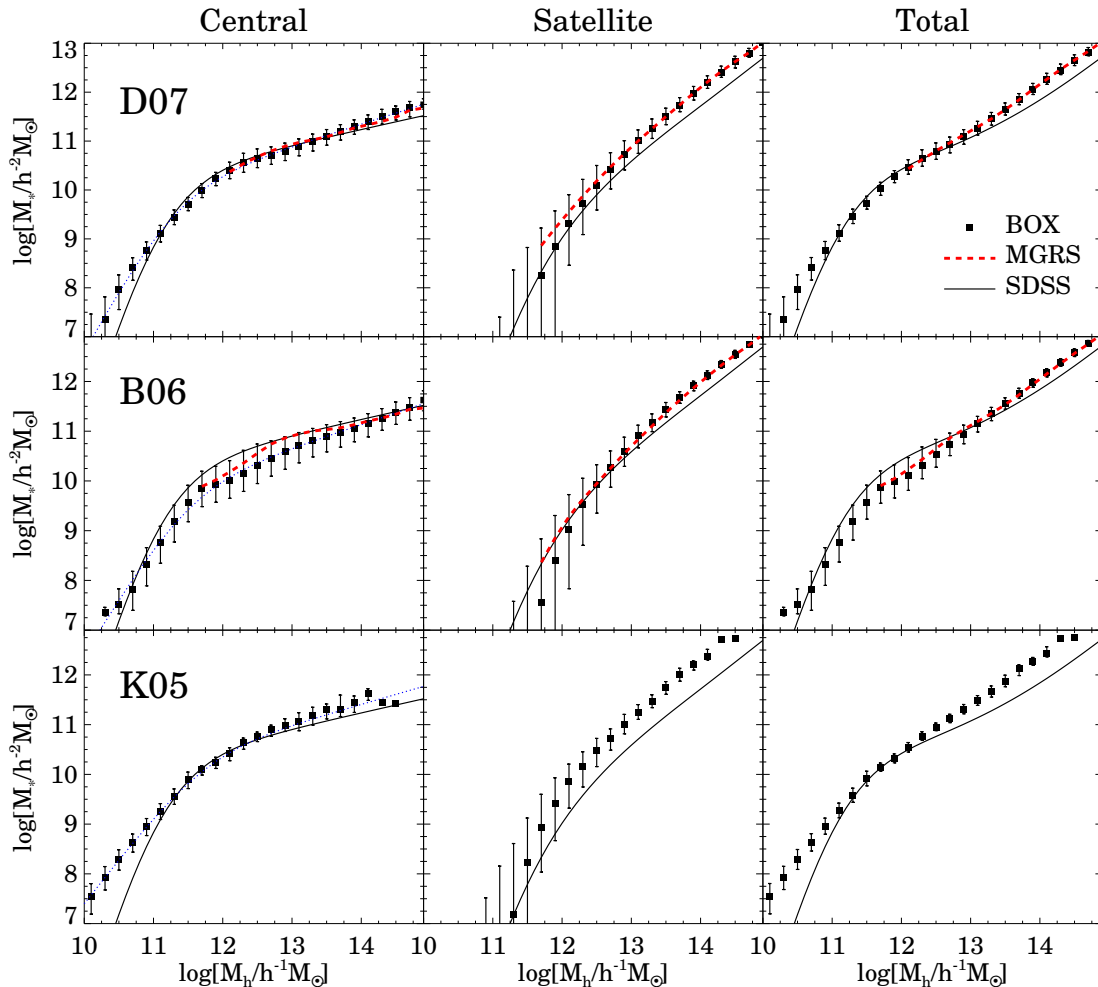
FIG. 2.— The total stellar masses of central, satellite and all galaxies in halos of different masses. Results from D07, B06 and K05 are shown as symbols with error bars, in the upper, middle and lower row panels, respectively. The error bars in this plot indicate the 84% confidence levels in different halo mass bins. For comparison, in each panel, the solid line shows the observational results obtained by Y09b from SDSS. The dotted lines shown in the left column panels are the best fit results for the SAMs. In the upper two rows of panels, results obtained from MGRSs (i.e. based on extracted groups) are shown as dashed lines.

are shown as solid squares with error bars (which indicate the corresponding 84% confidence levels). For comparison, we also show, in the upper two rows, the results obtained from the MGRSs (dashed lines). In general, the results obtained directly from the simulation boxes agree well with those obtained from the MGRS. This is extremely reassuring, as it implies that the results obtained from the Y07 galaxy group catalogue are reliable.

Let us first consider the central galaxies. As shown in Y09b, the conditional probability distribution, $\mathcal{P}_c(M_*|M_h)$, that a halo of mass M_h hosts a *central* galaxy with stellar mass M_* can be described by a log-normal distribution with the mean given by

$$\langle M_{*,c}\rangle(M_h) = M_0 \frac{(M_h/M_1)^{\alpha+\beta}}{(1+M_h/M_1)^{\beta}}. \qquad (10)$$

We use this relation to fit the stellar mass - halo mass relation of centrals predicted by the three SAMs. The best fit parameters are listed in Table 1, and the results are also shown in the left columns of Fig. 2 as the dotted lines. These results should be compared to the best fit

values obtained by Y09b for central galaxies in the SDSS group catalogue, shown in each panel as the solid line: the corresponding best fit parameters are also listed in Table 1. Note that the predictions of D07 and K05 for the stellar mass - halo mass relation are quite similar. Both models slightly over-predict the stellar mass of central galaxies in massive halos with $M_h \gtrsim 10^{14} h^{-1}M_\odot$, and severely over-predict the stellar masses in low mass halos ($M_h \lesssim 10^{11} h^{-1}M_\odot$). In the intermediate halo-mass range, both D07 and K05 match the observational data reasonably well. The B06 model yields a stellar mass - halo mass relation of central galaxies that is quite different: although it matches the data at both the massive ($M_h \sim 10^{14.5} h^{-1}M_\odot$) and low-mass ($M_h \sim 10^{11} h^{-1}M_\odot$) ends, it significantly under-predicts the stellar masses in intermediate-mass halos.

It is instructive to look at the best fit parameters listed in Table 1. As one can see, B06 predicts a lower characteristic stellar mass, M_0, than the other two models, which reflects an overall lower amplitude of the stellar mass - halo mass relation of central galaxies. Compared

to the SDSS data, the biggest discrepancy for all the three SAMs concerns the slope, β, at the low-mass end. The models predict $1.4 \lesssim \beta \lesssim 2.2$, much smaller than $\beta \sim 4.5$ obtained from the SDSS. This indicates that the star formation efficiency in low-mass halos increases with halo mass much faster than assumed in the SAMs. This is consistent with the results obtained by Mo et al. (2005), who found that it is difficult to reproduce the observed low-mass end of the stellar mass function if the star formation in low-mass halos is mainly regulated by supernova feedback, and by Pasquali et al. (2009b), who have demonstrated that typical SAMs significantly over-predict the stellar population ages of central galaxies in low mass halos.

Next we focus on the contribution of satellite galaxies to the stellar mass budget. The panels in the middle column of Fig. 2 show the total stellar mass contained in satellite galaxies as function of halo mass, defined as the sum of the stellar masses of all the member satellite galaxies with $M_* \geq 10^8 h^{-2}\,\mathrm{M_\odot}$. The solid line in each of the middle-column panels shows the observed average, obtained by Y09a, properly converted to this particular stellar mass limit of $10^8 h^{-2}\,\mathrm{M_\odot}$. Clearly, all three SAMs significantly over-predict the total stellar mass contained in satellites, especially in halos with $M_\mathrm{h} \gtrsim 10^{13}\,h^{-1}\mathrm{M_\odot}$.

Finally, the right-hand panels of Fig. 2 show the total stellar mass (central plus all satellites with $M_* \geq 10^8 h^{-2}\,\mathrm{M_\odot}$) as function of halo mass. Compared to the SDSS data, D07 and K05 significantly over-predict the total stellar masses in halos at both the high- and low-mass ends. On the other hand, B06 also over-predicts the total stellar mass in massive halos, but under-predicts the total stellar mass in halos with $10^{11}\,h^{-1}\mathrm{M_\odot} \lesssim M_\mathrm{h} \lesssim 10^{12.5}\,h^{-1}\mathrm{M_\odot}$. It is clear that the discrepancy at the low-mass end is due to centrals, while that at the high-mass end is due to satellites.

5.3. The conditional stellar mass functions

To get more insight regarding the origin of the discrepancies between model predictions and data, we now examine the conditional stellar mass function (CSMF), $\Phi(M_*|M_\mathrm{h})$, which describes the average number of galaxies of stellar mass M_* that reside in a halo of mass M_h. The CSMF has been measured directly from the SDSS galaxy group catalogue by Y09b. For the three SAMs considered here, we determine the CSMFs separately for central and satellite galaxies directly from the simulation boxes, and for B06 and D07 also from the group catalogues constructed from their corresponding MGRSs. The results of the direct measurements are shown as the solid lines in Figs. 3, 4 and 5 for D07, B06 and K05, respectively, while those obtained from the MGRS are shown as dashed lines (in Figs. 3 and 4 only). In each panel, the symbols with error bars indicate the observational results of Y09b.

Let us first focus on the CSMFs for central galaxies. In D07, we see that the mock group results agree very well with the direct measurements, although the former yield a width that is somewhat smaller than the true width, obtained directly from the simulation boxes, in low mass halos. In the case of the B06 model, however, there is a huge discrepancy between the CSMF of central galaxies obtained from the mock group results and that obtained directly from the simulation boxes. In particular, the

width of the former is much smaller than that of the latter, indicating that the width of the CSMF obtained from our SDSS galaxy group catalogue may be substantially underestimated. As discussed in Y09b, this is due to the fact that the assignment of halo masses to the groups assumes zero scatter in the M_*-M_h relation. If the true M_*-M_h relation contains a large amount of scatter, as is the case for the B06 model, this results in significant errors in the assigned halo masses, and a significant underestimate of the width of the CSMF for centrals. Hence, the width obtained from the galaxy group catalogues has to be considered a lower limit on the true width.

It is clear from a comparison of Figs 3, 4 and 5 that the B06 model predicts a much larger scatter in the stellar masses of central galaxies than the D07 and K05 models, especially in low mass halos[7]. It is therefore important to obtain constraints on the true amount of scatter in the M_*-M_h relation of central galaxies. It should be clear from the above, that we cannot use the SDSS group catalogue for this. After all, we obtain similar widths for the CSMFs of centrals when we apply our group finder to the D07 and B06 MGRSs, even though their intrinsic widths are clearly very different. However, recently More et al. (2009) have constrained the scatter, $\sigma_{\log M_*}$, as a function of halo mass using satellite kinematics. Their method, which has been tested using detailed mock galaxy redshift surveys, indicate that $\sigma_{\log M_*} \sim 0.16$ dex. A similar amount of scatter was inferred by Cacciato et al. (2009) from an analysis of the galaxy-galaxy lensing signal in the SDSS, as measured by Seljak et al. (2005) and Mandelbaum et al. (2006). Taking these observational constraints at face value, they clearly rule out the huge amount of scatter predicted by the B06 model. Interestingly, though, it is in excellent agreement with the amounts of scatter predicted by both the D07 and K05 models.

Focusing on the peak positions of the CSMFs of central galaxies, rather than the scatter, we notice the same discrepancies as in Fig. 2: the D07 and K05 models over-predict the mean stellar mass of central galaxies in massive halos, while B06 under-predicts the mean stellar mass of central galaxies in halos with $M_\mathrm{h} \sim 10^{12} h^{-1}\,\mathrm{M_\odot}$.

For satellite galaxies, the overall mock group results agree reasonably well with the direct measurements[8]. However, the CSMF for the mock groups in relatively massive halos is slightly overestimated, and in relatively small halos slightly underestimated especially at the massive end. Note that, in a mock group, the most massive galaxy is always defined to be the central galaxy. Thus, if the true central is not the most massive one (i.e. one or more satellites are more massive than the central), the mass of the most massive satellite is underestimated, leading to an underestimate of the conditional stellar mass function at the massive end. Furthermore, the masses of some mock groups may be over-estimated by the ranking of their stellar masses if their stellar masses are exceptionally large. Because of these uncertainties, it is perhaps more meaningful to compare the observa-

---

[7] Although the origin of this dramatic difference is not entirely clear to us, we believe that it originates from the way B06 implement AGN feedback.

[8] The abrupt truncation in the CSMF obtained from the D07 MGRS apparent in the lower-left panel of Fig. 3 is a manifestation of cosmic variance.
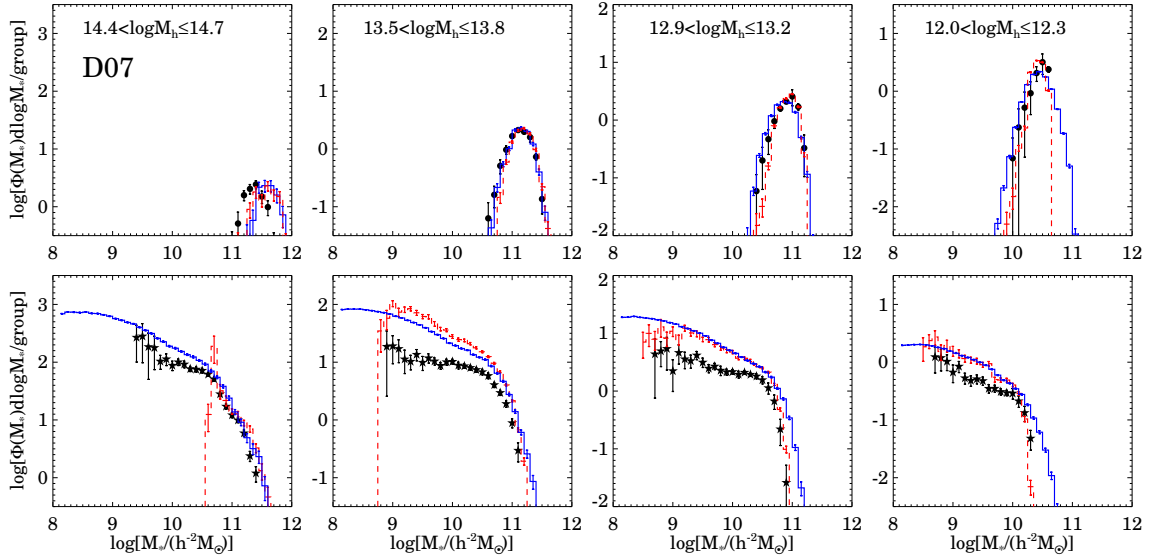
FIG. 3.— The conditional stellar mass functions (CSMFs) of galaxies in halos of different mass bins. Shown in the upper panels are results for central galaxies, while the lower panels give results for satellite galaxies. Symbols with error are for the SDSS observational results, whereas the histograms with error bars show the SAM predictions of D07. The blue solid histograms are obtained directly for the raw models in a cubic box, whereas the red dashed ones are obtained for groups extracted for MGRSs. The error bars for the SAM predictions are obtained using 500 bootstrap resamplings.
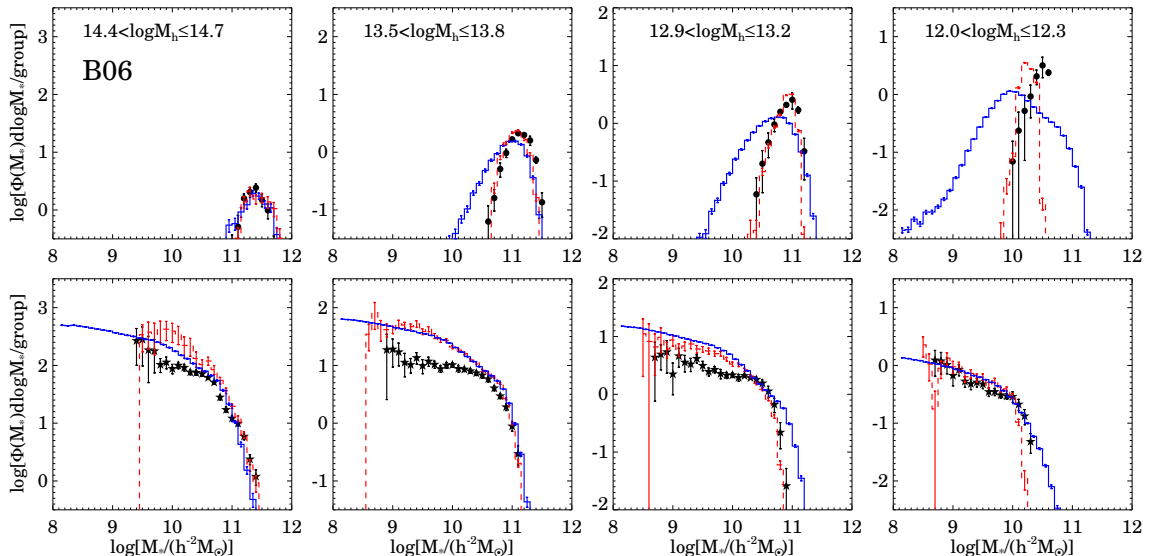
FIG. 4.— Similar to Fig. 3 but for the SAM predictions of B06.

tional results with the results obtained from the MGRS. As one can see, all the SAMs over-predict the CSMF of satellites at the faint end, especially in relatively massive halos.

6. WHAT IS MISSING IN SEMI-ANALYTICAL MODELS?

The model-data comparisons presented in the previous section show that all three SAMs considered fail in the following two aspects. First, the models over-predict the number of satellite galaxies by about a factor of two, for halos of all masses. Second, the predicted stellar mass - halo mass relation of central galaxies is too shallow at the low-mass end. In this section we investigate how these

problems may be remedied.

In all three SAMs considered above, once a halo is accreted by a larger halo, its galaxies (now 'satellite galaxies') are assumed to either merge with the central galaxy of the host halo or to remain as individual satellite galaxies in their new host halo (but see a recent attempt by Henriques & Thomas 2009 who have introduced into the SAM by D07 the tidal stripping of stellar material from satellite galaxies during mergers). Other possibilities, such as satellite-satellite merging, and the stripping and disruption of satellites due to tidal forces, are not taken into account. However, both processes are believed to play an important role. In fact, numerous studies in recent years have argued that reconciling
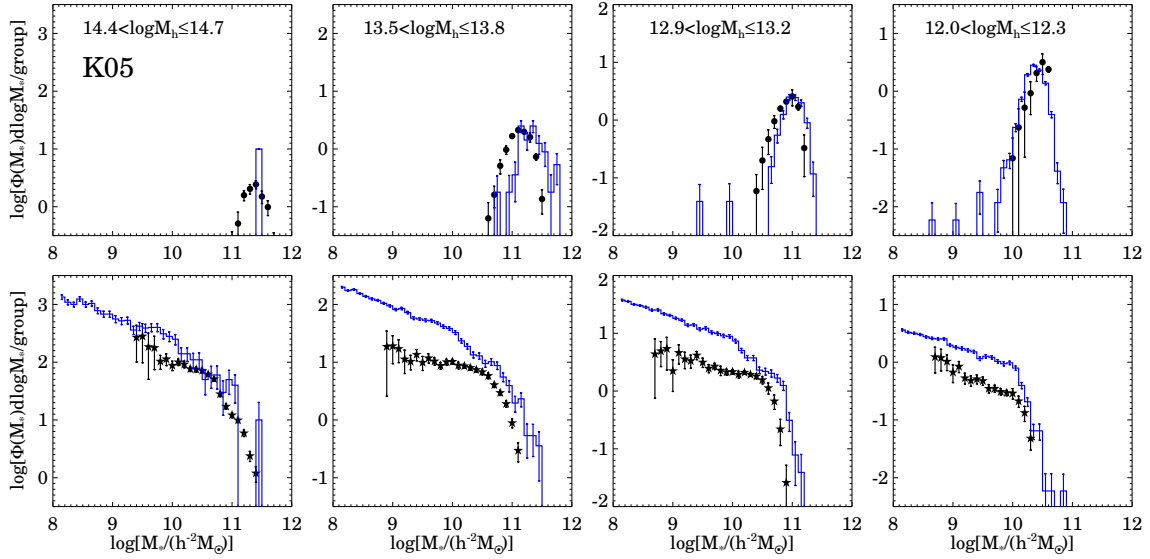
Fig. 5.— Similar to Fig. 3 but for the SAM predictions of K05. Note that we do not have results based on a MGRS for this model.
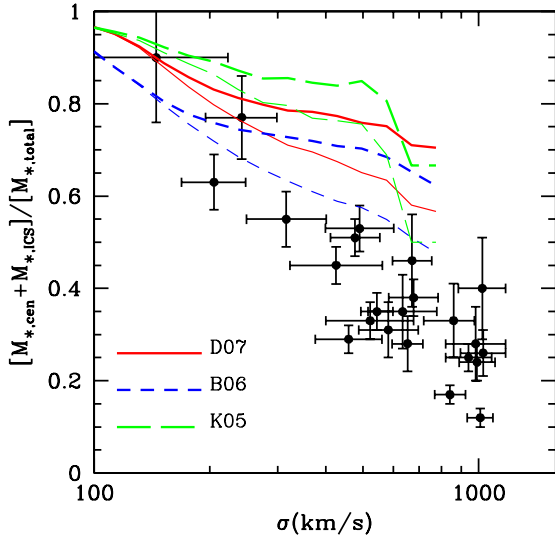

Fig. 6.— The fraction of the total stellar mass contained in the central galaxy and in intra-cluster stars as a function of cluster velocity dispersion. Data with error bars are obtained from Gonzalez et al. (2007), measured within r_{500} for the 23 groups and clusters in their sample. The solid, dashed and long-dashed lines are model predictions for D07, B06 and K05, respectively. The thick and thin lines correspond to the two extreme cases we analyzed (see text for details).

halo occupation statistics with halo merger rates requires that a significant fraction of satellite galaxies is indeed tidally disrupted (e.g., Conroy, Ho & White 2007; Conroy, Wechsler & Kravtsov 2007; Kang & van den Bosch 2008; Y09a). In addition, Kim et al. (2009) have argued that both tidal disruption and satellite-satellite merging are required in order to reproduce the two-point correlation function of galaxies on small scales. Since satellite-satellite merging does not reduce the total stellar mass in the host halo, and so cannot alleviate the discrepancy between model and data shown in the right panels of Fig. 2, in what follows we focus on the impact of tidal stripping.

As shown in the panels in the middle column of Fig. 2, all three SAMs over-predict the *total* stellar mass of satellites in halos with $M_h \gtrsim 10^{13.0} h^{-1} M_\odot$. In order to reduce the amount of stellar mass locked up in satellite galaxies without changing the star formation prescription in the models, a significant fraction of the stars in satellite galaxies has to be stripped and form the stellar halos and intra-cluster stars (ICS)[9] observed in our Milky Way halo, in groups and clusters, and around isolated galaxies (e.g., Helmi et al. 1999; Ferguson et al. 2002; Yanny et al. 2003; Zibetti, White & Brinkmann 2004; Gonzalez, Zabludoff & Zaritsky 2005, 2007; Seigar, Graham & Jerjen 2007; Bell et al. 2008). In addition, recent hydrodynamical simulations also suggest a very significant fraction of ICS in clusters of galaxies. (Puchwein et al. 2010). As a quantitative measure of how many stars are observed in the form of ICS, the solid dots with errorbars in Fig. 6 show the observed fraction of the total stellar mass present in groups and clusters that is contained in the central galaxy and the ICS as a function of the line-of-sight velocity dispersion of member galaxies. These data are taken from Gonzalez et al. (2007), under the assumption that satellite galaxies, central galaxies and the ICS all have a similar stellar mass-to-light ratio (in the i-band). We compare the observational data with the predictions of the three SAMs: D07 (solid lines), B06 (dashed lines) and K05 (long-dashed lines), assuming that the entire excess of stellar mass in satellite galaxies predicted by the models resides in ICS. Here the halo mass is converted into a line-of-sight velocity dispersion using equation (6) in Yang et al. (2007). Note that the data of Gonzalez et al. (2007) are obtained within r_{500}, the radius within which the cluster mass density exceeds the critical value by a factor of 500. This factor has been taken into account in all the three SAM predictions: the total mass of satellite galaxies within r_{500} is estimated by assuming that the distribution of satellite galaxies

---

[9] Throughout this paper we will use the terms 'ICS' and 'stellar halo' without distinction.

follows the NFW (Navarro, Frenk & White 1997) profile with concentration appropriate for the halo mass in question. For the distribution of ICS, we consider two cases. Case I assumes that the ICS have the same distribution as the satellite galaxies, and the corresponding results are shown in Fig. 6 as the three thin lines. Case II assumes that all ICS are distributed within r_{500}, and the corresponding results are shown in Fig. 6 by the three thick lines. Except perhaps for the Case I scenario of B06, all model predictions thus obtained significantly over-predict the ratio $[M_{*,\mathrm{cen}} + M_{*,\mathrm{ICS}}]/M_{*,\mathrm{total}}$ in massive halos. This suggests that all models predict too many stars, and that a consistent result cannot be obtained without changing the prescription for star formation. This is further corroborated by the fact that the observational estimates by Gonzalez et al. (2007) for the ICS component lie at the upper end of the reported values, with other studies finding considerably lower numbers (e.g. Zibetti, White & Brinkmann, 2004).

As one can see from Figs. 3 to 5, the main problem arises because the models predict too many low-mass satellite galaxies, especially in relatively massive halos. Since satellite galaxies were central galaxies before they were accreted by their host halos, this discrepancy suggests that the star formation efficiency in low-mass halos needs to be reduced in the SAMs. This is further supported by the fact that the SAMs predict a low-mass end slope β for the stellar mass - halo mass relation of central galaxies that is much too shallow (see section 5.2) and by the fact that SAMs typically over-predict the mass-weighted stellar ages of low-mass galaxies (Pasquali et al. 2009b). Furthermore, as recently demonstrated in Y09a, if one assumes that the central stellar mass - halo mass relation is independent of redshift (see also Wang et al. 2006), then a model that can reproduce the observed stellar mass - halo mass relation of centrals can also reproduce the observed stellar mass function of satellite galaxies and the observed ICS. All these results clearly suggest that current semi-analytical models over-predict the star formation efficiencies in low mass halos.

7. SUMMARY

We have evaluated three SAMs by De Lucia & Blaizot (2007; D07), Bower et al. (2006; B06) and Kang et al. (2005; K05), using observational measurements of the stellar mass functions, the total stellar mass in halos of different masses, and the conditional stellar mass functions for central and satellite galaxies. Our results can be summarized as follows.

- All three SAMs predict stellar mass - halo mass relations of central galaxies that have a similar shape, but a different normalization. While D07 and K05 over-predict the stellar masses of centrals in massive and low mass halos, B06 under-predict the stellar masses of centrals in intermediate mass halos. None of the SAMs reproduces the observed steep slope of this relation at the low-mass end.

- All three SAMs over-predict the ratio of the stellar mass functions of satellites and centrals, $\Phi_{\mathrm{s}}(M_*)/\Phi_{\mathrm{c}}(M_*)$, by about a factor of two at all M_*.

- All three SAMs over-predict the total stellar mass

and number of low-mass satellite galaxies, especially in massive halos.

Neither of the three SAMs considered here takes account of tidal stripping of (the stellar components of) satellite galaxies. Rather, satellite galaxies either survive to the present day with roughly the same stellar mass as they has at their epoch of accretion, or they are accreted by the central galaxy in their host halo. Whether a satellite survives or is accreted is determined by the efficiency of dynamical friction, which controls the rate at which the satellite loses its momentum. In reality, however, satellite galaxies are expected to experience tidal stripping, which not only increases their dynamical friction times, but also may cause satellite galaxies to be tidally disrupted. In either case, a certain fraction of the stars originally associated with satellite galaxies ends up being associated with a stellar halo (called 'intra-cluster stars' in the case where the host halo is cluster-sized). Hence, one can improve the problem with the overproduction of stellar mass associated with satellite galaxies, by assuming that a certain fraction of satellite galaxies are tidally stripped or disrupted. However, we have shown that the amount of stripping required in the SAMs in order to match the observed conditional stellar mass function of satellites would significantly over-predict the mass of the ICS-component in massive halos compared with observation. This indicates that the problem with the stellar masses of satellite galaxies is not solely a consequence of how the models treat the evolution of satellite galaxies. Rather, we argue that the satellite galaxies in the SAMs are too massive because they were already too massive at their time of accretion, when they were still centrals. This is supported by the fact that the models also fail to reproduce the low-mass end slope of the stellar mass - halo mass relation of centrals. We therefore conclude that SAMs over-predict the star formation efficiencies in low mass halos.

The main mechanism that is invoked in (semi-analytical) models of galaxy formation in order to regulate the star formation efficiency in low mass halos is supernova (SN) feedback. Hence, a naive solution to the problems identified here seems to be to simply increase the supernova feedback efficiency, typically expressed in terms of the fraction of supernova energy used to either expel or reheat cold gas. However, often this efficiency is already taken to be unrealistically high. For example, in the B06 model it is larger than unity in halos with a circular velocity less than $200\,\mathrm{km\,s^{-1}}$ (see Benson et al. 2003 for a detailed discussion). Another problem with supernova feedback as the only mechanism to suppress star formation in low mass halos is that it requires star formation, which in turn requires high surface densities of gas. As shown in Mo et al. (2005), the cold gas mass fractions required in order to maintain the needed level of SN feedback are too high compared to observation.In addition, strong supernova feedback can lead to overly low effective metal yields, resulting in metallicities in low mass galaxies that are too low. Hence, it is unlikely that a mere modification of SN feedback can solve the stellar mass problems identified in this paper, suggesting that other forms of feedback, perhaps from AGN in the quasar mode (Di Matteo, Springel & Hernquist 2005), are needed. An alternative solution is that the in-

tergalactic medium (IGM) is preheated so that the total amount of gas that can be accreted by a low mass halo for star formation is reduced (Mo & Mao 2002). However, at the moment there is no direct evidence to support the idea that the (high-redshift) IGM may have been substantially pre-heated. We therefore conclude that we still lack a proper understanding of the mechanisms that regulate star formation in low mass halos.

REFERENCES

Adelman-McCarthy J. K. et al. , 2006, ApJS, 162, 38
Baldry I. K., Balogh M. L., Bower R. G., Glazebrook K., Nichol R. C., Bamford S. P., & Budavari T., 2006, MNRAS, 373, 469
Bell E. F., McIntosh D. H., Katz N., & Weinberg M. D., 2003, ApJS, 149, 289
Bell E. F., et al., 2008, ApJ, 680, 295
Benson A. J., Cole S., Frenk C. S., Baugh C. M., & Lacey C. G., 2000, MNRAS, 316, 107
Benson A. J., Lacey C. G., Baugh C. M., Cole S., Frenk C. S., 2002, MNRAS, 333, 156
Benson A. J., Bower R. G., Frenk C.S., Lacey C. G., Baugh C. M., & Cole S., 2003, ApJ, 599, 38
Blanton M. R. et al. , 2005, AJ, 129, 2562
Blanton M. R., Roweis S., 2007, AJ, 133, 734
Bower R. G., Benson A. J., Malbon R., Helly J. C., Frenk C. S., Baugh C. M., Cole S., & Lacey C. G., 2006, MNRAS, 370, 645 (B06)
Cacciato M., van den Bosch F.C., More S., Ran L., Mo H. J., & Yang X., 2009, MNRAS, 394, 929
Cattaneo A., Dekel A., Devriendt J., Guiderdoni B., & Blaizot J., 2006, MNRAS, 370, 1651
Chabrier G., 2003, PASP, 115, 763
Cole S., Aragón-Salamanca A., Frenk C. S., Nararro J. F., & Zepf S. E., 1994, MNRAS, 271, 781
Cole S., Lacey C. G., Baugh C. M., & Frenk C. S., 2000, MNRAS, 319, 168
Collister A.A., & Lahav O., 2005, MNRAS, 361, 415
Conroy C., Ho S., White M., 2007, MNRAS, 379, 1491
Conroy C., Wechsler R. H., Kravtsov A. V., 2007, ApJ, 668, 826
Cooray A., 2006, MNRAS, 365, 842
Cox T. J., Primack J., Jonsson P., Somerville R. S., 2004, ApJ, 607, L87
Croton D. J., Springel V., White S. D. M., De Lucia G., Frenk C. S., Gao L., Jenkins A., Kauffmann G., Navarro J. F., & Yoshida N., 2006, MNRAS, 365, 11C
De Lucia G., Blaizot J., 2007, MNRAS, 375, 2 (D07)
De Lucia G., Springel V., White S. D. M., Croton D., Kauffmann G., 2006, MNRAS, 366, 499
Di Matteo T., Springel V., Hernquist L., 2005, Nature, 433, 604
Ferguson A. M. N., Irwin M. J., Ibata R. A., Lewis G. F., Tanvir N. R., 2002, AJ, 124, 1452
Font A. S. et al., 2008, MNRAS, 389, 1619
Fontanot F., De Lucia G., Monaco P., Somerville R. S., & Santini P., 2009, MNRAS, 987
Fukugita M., Ichikawa T., Gunn J. E., Doi M., Shimasaku K., Schneider D. P., 1996, AJ, 111, 1748
Gnedin N. Y., 2000, ApJ, 542, 535
Gonzalez A. H., Zaritsky D., Zabludoff A. I., 2005, ApJ, 618, 195
Gonzalez A. H., Zaritsky D., Zabludoff A. I., 2007, ApJ, 666, 147
Helly J. C., Cole S., Frenk C. S., Baugh C. M., Benson A., & Lacey C., 2003, MNRAS, 338, 903
Helmi A., White S. D. M., de Zeeuw P. T., Zhao H., 1999, Nature, 402, 53
Henriques B., Bertone S., & Thomas P.A., 2008, MNRAS, 383, 1649
Henriques B. M. B., & Thomas, P. A. 2009, arXiv:0909.2150
Jing Y. P., Mo H. J., & Börner G., 1998, ApJ, 494, 1
Jing Y. P., & Suto Y., 2002, ApJ, 574, 538
Kang X., Jing Y. P., Mo H. J., Börner G., 2005, ApJ, 631, 21 (K05)
Kang X., & van den Bosch F.C., 2008, ApJ, 676, L101
Kauffmann G., Colberg J. M., Diaferio A., & White S. D. M., 1999, MNRAS, 303, 188
Kauffmann G., Haehnelt M., 2000, MNRAS, 311, 576
Kauffmann G., White S. D. M., & Guiderdoni B., 1993, MNRAS, 264, 201
Kennicutt R. C., 1983, ApJ, 272, 54

Kim H. S., Baugh C. M., Cole S., Frank C. S., Benson A. J., 2009, arXiv:0905.4723
Kimm T., et al., 2009, MNRAS, 394, 1131
Kroupa P., 2001, MNRAS, 322, 231
Lacey C., & Silk, J. 1991, ApJ, 381, 14
Li C., Jing Y. P., Kauffmann G., Böerner, Kang X., Wang L., 2007, MNRAS, 376, 984
Lin W. P., Jing Y. P., Mao S., Gao L., McCarthy I. G., 2006, ApJ, 651, 636
Mandelbaum R., Seljak U., Kauffmann G., Hirata C. M., Brinkmann J., 2006, MNRAS, 368, 715
Malbon R. K., Baugh C. M., Frenk C. S., Lacey C. G., 2007, MNRAS, 382, 1394
McCarthy I. G., Frenk C.S., Font A. S., Lacey C., Bower R. G., Mitchell N. L., Balogh M. L., & Theuns T., 2008, MNRAS, 383, 593
Mo H. J., Mao S., 2002, MNRAS, 333, 768
Mo H. J., Mao S., White S. D. M., 1998, MNRAS, 295, 319
Mo H. J., Yang X., van den Bosch F.C., Katz N., 2005, MNRAS, 363, 1155
Monaco P., Fontanot F., & Taffoni G., 2007, MNRAS, 375, 1189
More S., van den Bosch F.C., Cacciato M., Mo H. J., Yang X., Ran L., 2009, MNRAS, 392, 801
Navarro J. F., Frenk C. S., & White S. D. M., 1997, ApJ, 490, 493
Neistein E., & Weinmann S.M., 2009, preprint (arXiv:0911.3147)
Pasquali A., van den Bosch F. C., Mo H. J., Yang X., & Somerville R. S., 2009, MNRAS 394, 38
Pasquali A., Gallazzi A., Fontanot F., van den Bosch F. C., De Lucia G., Mo H. J., & Yang X., 2009b, in preparation
Puchwein E., Springel V., Sijacki D. & Dolag K., 2010, arXiv:1001.3018
Scranton R., 2003, MNRAS, 339, 410
Seigar M. S., Graham A. W., Jerjen H., 2007, MNRAS, 378, 1575
Seljak U., et al., 2005, Phys. Rev. D., 71, 043511
Skibba R., 2009, MNRAS, 392, 1467
Somerville R. S., & Primack J. R., 1999, MNRAS, 310, 1087
Somerville R. S., Primack J. R., & Faber S. M., 2001, MNRAS, 320, 504
Somerville R. S., Hopkins P. F., Cox T. J., Robertson B. E., & Hernquist L., 2008, MNRAS, 391, 481
Spergel D. N., et al., 2007, ApJS, 170, 377
Springel V., 2005a, MNRAS, 364, 1105
Springel V. et al. , 2005b, Nat, 435, 629
Springel V., White S. D. M., Tormen G. & Kauffmann G., 2001, MNRAS, 328, 726
Tinker J. L., Weinberg D. H., Zheng Z., & Zehavi I., 2005, ApJ, 631, 41
Tinker J. L., & Wetzel A. R., 2009, arXiv:0909.1325
Vale A., & Ostriker J. P., 2004, MNRAS, 353, 189
van den Bosch F. C., 1998, ApJ, 507, 601
van den Bosch F. C., Yang X., & Mo H. J., 2003, MNRAS, 340, 771
van den Bosch F. C., Yang X., Mo H. J., Weinmann S. M., Maccio A., More S., Cacciato M., Skibba R., & Kang X., 2007, MNRAS, 376, 841
van den Bosch F. C., Aquino D., Yang X., Mo H. J., Pasquali A., McIntosh D. H., Weinmann S. M., & Kang X., 2008, MNRAS, 387, 79
Wang L., Li C., Kauffmann G., De Lucia G., 2006, MNRAS, 371, 537
Wang J., De Lucia G., Kitzbichler M. G., & White S. D. M., 2008, MNRAS, 384, 1301
Weinmann S. M., van den Bosch F. C., Yang X., & Mo H. J., 2006a, MNRAS, 366, 2
Weinmann S. M., van den Bosch F. C., Yang X., Mo H. J., Croton D. J., & Moore B., 2006b, MNRAS, 372, 1161

Weinmann S. M., Kauffmann G., van den Bosch F. C., Pasquali A., McIntosh D.H., Mo H. J., Yang X., & Guo Y., 2009, MNRAS, 394, 1213

White S. D. M., & Frenk C. S. 1991, ApJ, 379, 52

Yang X., Mo H. J., Jing Y. P., van den Bosch F. C., 2005b, MNRAS, 358, 217

Yang X., Mo H. J., Jing Y. P., van den Bosch F. C., Chu Y. Q., 2004, MNRAS, 350, 1153

Yang X., Mo H. J., van den Bosch F. C., 2003, MNRAS, 339, 1057

Yang X., Mo H. J., van den Bosch F. C., 2008, ApJ, 676, 248

Yang X., Mo H. J., van den Bosch F. C., 2009, ApJ, 693, 830 (Y09a)

Yang X., Mo H. J., van den Bosch F. C., 2009, ApJ, 695, 900 (Y09b)

Yang X., Mo H. J., van den Bosch F. C., Jing Y. P., 2005a, MNRAS, 356, 1293

Yang X., Mo H. J., van den Bosch F. C., Pasquali A., Li C., Barden M., 2007, ApJ, 671, 153

Yanny B., et al., 2003, ApJ, 588, 824

Zehavi I., et al., 2002, ApJ, 571, 172

Zehavi I., et al., 2004, ApJ, 608, 16

Zehavi I., et al., 2005, ApJ, 630, 1

Zheng Z., Berlind A. A., Weinberg D. H., Benson A. J., Baugh C. M., Cole S., Davé R., Frenk C. S., Katz N., & Lacey C. G., 2005, ApJ, 633, 791

Zheng Z., Coil A. L., & Zehavi I., 2007, ApJ, 667, 760

Zibetti S., White S. D. M., Brinkmann J., 2004, MNRAS, 347, 556